








Communication

# Exploiting Integrin- $\alpha$ V $\beta$ 3 to Enhance Radiotherapy Efficacy in Medulloblastoma via Ferroptosis

Célia Gotorbe <sup>1</sup>, Fabien Segui <sup>1</sup>, William Echavidre <sup>1</sup>, Jérôme Durivault <sup>1</sup> , Thays Blanchard <sup>1</sup>, Valérie Vial <sup>1</sup> , Marina Pagnuzzi-Boncompagni <sup>1</sup>, Rémy Villeneuve <sup>2</sup> , Régis Amblard <sup>2</sup>, Nicolas Garnier <sup>2</sup>, Cécile Ortholan <sup>3</sup>, Benjamin Serrano <sup>2</sup> , Vincent Picco <sup>1</sup> , Jacques Pouyssegur <sup>1,4</sup> , Milica Vucetic <sup>1,\*</sup> and Christopher Montemagno <sup>1,\*</sup> 

<sup>1</sup> Biomedical Department, Centre Scientifique de Monaco, 98000 Monaco, Monaco; cgotorbe@centrescientifique.mc (C.G.); fsegui@centrescientifique.mc (F.S.); wechavidre@centrescientifique.mc (W.E.); jdurivault@centrescientifique.mc (J.D.); thaysblanchard98@gmail.com (T.B.); vial@centrescientifique.mc (V.V.); mpagnuzzi@centrescientifique.mc (M.P.-B.); vpicco@centrescientifique.mc (V.P.); jacques.pouyssegur@univ-cotedazur.fr (J.P.)

<sup>2</sup> Radiophysics Department, Princess Grace Hospital, 98000 Monaco, Monaco; remy.villeneuve@chpg.mc (R.V.); regis.amblard@chpg.mc (R.A.); nicolas.garnier@chpg.mc (N.G.); benjamin.serrano@chpg.mc (B.S.)

<sup>3</sup> Radiotherapy Department, Princess Grace Hospital, 98000 Monaco, Monaco; cecile.ortholan@chpg.mc

<sup>4</sup> CNRS, INSERM, Centre A. Lacassagne, Institute for Research on Cancer & Aging (IRCAN), University Côte d'Azur, 06107 Nice, France

\* Correspondence: milica@centrescientifique.mc (M.V.); cmontemagno@centrescientifique.mc (C.M.); Tel.: +377-97-77-44-21 (M.V.); +377-97-77-44-10 (C.M.)

**Abstract:** Medulloblastoma, a malignant pediatric brain tumor, has a poor prognosis upon relapse, highlighting a critical clinical need. Our previous research linked medulloblastoma cell radioresistance to integrin- $\alpha$ V $\beta$ 3 expression.  $\beta$ 3-depleted ( $\beta$ 3\_KO) medulloblastoma cells exhibit lipid hydroperoxide accumulation after radiotherapy, indicating ferroptosis, a regulated cell death induced by ROS and inhibited by antioxidants such as cysteine, glutathione (GSH), and glutathione peroxidase 4 (GPx4). However, the link between  $\alpha$ V $\beta$ 3 expression, ferroptosis inhibition, and sensitivity to radiotherapy remains unclear. We showed that irradiated  $\beta$ 3\_KO medulloblastoma cells primarily die by ferroptosis, with  $\beta$ 3-subunit expression correlating with radiotherapy sensitivity and anti-ferroptotic protein levels. Our findings suggest that integrin- $\alpha$ V $\beta$ 3 signaling boosts oxidative stress resilience via mTORC1. Thus, targeting integrin- $\alpha$ V $\beta$ 3 could enhance radiotherapy efficacy in medulloblastoma by inducing ferroptotic cell death.

**Keywords:** integrin- $\alpha$ V $\beta$ 3; medulloblastoma; cilengitide; radiotherapy; ferroptosis



**Citation:** Gotorbe, C.; Segui, F.; Echavidre, W.; Durivault, J.; Blanchard, T.; Vial, V.; Pagnuzzi-Boncompagni, M.; Villeneuve, R.; Amblard, R.; Garnier, N.; et al. Exploiting Integrin- $\alpha$ V $\beta$ 3 to Enhance Radiotherapy Efficacy in Medulloblastoma via Ferroptosis. *Curr. Oncol.* **2024**, *31*, 7390–7402. <https://doi.org/10.3390/curroncol31110545>

Received: 20 September 2024  
Revised: 31 October 2024  
Accepted: 7 November 2024  
Published: 20 November 2024



**Copyright:** © 2024 by the authors. Licensee MDPI, Basel, Switzerland. This article is an open access article distributed under the terms and conditions of the Creative Commons Attribution (CC BY) license (<https://creativecommons.org/licenses/by/4.0/>).

## 1. Introduction

Medulloblastoma (MB) is one of the most common malignant brain tumors in children, accounting for 20% of pediatric central nervous system (CNS) tumors [1]. Since 2016, the World Health Organization (WHO) has classified MB as a grade IV tumor based on its malignancy and treatment challenges—an unchanged classification [2,3]. The standard treatment for MB involves surgical resection followed by craniospinal irradiation and adjuvant chemotherapy [4,5]. While these treatments have significantly improved patient survival rates, they are associated with severe side effects, including neurological deficits and neurocognitive impairments [6]. Additionally, relapse occurs in about 30% of cases, leading to a poor prognosis [7–9]. Therefore, improving current therapies is critical, especially considering the young age of the affected patients.

Radiotherapy is a cornerstone of treatment, yet the recurrence observed in patients highlights the radioresistance of MB. An effective therapeutic strategy to address this challenge could involve enhancing the cytotoxic effect of radiotherapy on tumor cells by

targeting key factors involved in radioresistance [10–12]. Our previous study identified integrin- $\alpha v \beta 3$  as a crucial player in MB's radioresistance [13]. Integrins are a superfamily of adhesion proteins involved in cell-extracellular matrix (ECM) interactions, consisting of 18  $\alpha$ -subunits and eight  $\beta$ -subunits forming at least 24 different receptors [14]. Integrin interactions with ECM components trigger intracellular signaling pathways that regulate cell growth and survival under physiological conditions. However, dysregulated integrin expression in various cancers, including brain tumors, leads to enhanced signaling that promotes uncontrolled proliferation and aberrant angiogenesis [15,16]. Among integrins, integrin- $\alpha v \beta 3$  is highly expressed and crucial for the invasiveness of brain tumors. Its role has been extensively studied in glioblastoma, where its expression correlates with tumor grade, promotes angiogenesis, and facilitates cancer cell adhesion to the ECM and dissemination throughout the brain [16]. Similarly, our research demonstrated that integrin- $\alpha v \beta 3$  is significantly expressed in a subpopulation of MB patients, and  $\beta 3$ -subunit deletion impairs the tumorigenic capacities of MB. Moreover, integrin- $\alpha v \beta 3$  was associated with the radioresistance of MB cells. Notably, we observed that  $\beta 3$ -depleted cells exhibited a distinct bubbling phenotype characteristic of ferroptosis upon radiation exposure. Ferroptosis is a regulated, ROS- and iron-dependent form of cell death involving oxidative damage to plasma membrane lipids [17]. The canonical anti-ferroptotic pathway involves the cystine transporter (xCT), glutathione (GSH), and glutathione peroxidase 4 (GPX4), which detoxify lipid hydroperoxides. GPX4, a key player in this pathway, uses GSH to reduce lipid hydroperoxides to less toxic alcohol derivatives, with its activity dependent on cysteine import via the xCT transporter [18–20]. However, the relationship between radiotherapy-induced ferroptosis and integrin- $\alpha v \beta 3$  and the connection between MB and ferroptosis has not yet been explored. In this study, we aimed to assess the role of integrin- $\alpha v \beta 3$  in this process. First, we confirmed that ferroptosis is the predominant cell death pathway in  $\beta 3$ -depleted MB cells following radiotherapy. Our analysis revealed that the increased sensitivity of these cells to radiation-induced ferroptosis is due to lower levels of antioxidant defenses, particularly GPX4 protein content, compared to their WT counterparts. The basal GPX4 content was lower in  $\beta 3$ -depleted cells and remained low even after irradiation. We hypothesized that integrin- $\alpha v \beta 3$  signaling controls GPX4 protein synthesis via the mTORC1 pathway. Our data were confirmed with the use of cilengitide, a pharmacological inhibitor of integrin- $\alpha v \beta 3$  that enhances radiotherapy-induced ferroptosis. Therefore, integrin- $\alpha v \beta 3$  is a promising therapeutic target for MB as an antitumoral agent and a sensitizer to ROS-inducing treatments. To the best of our knowledge, this is the first study that demonstrates the impact of integrin- $\alpha v \beta 3$  in the mitigation of radiotherapy-induced ferroptosis.

## 2. Materials and Methods

### 2.1. Chemicals

Different chemicals were used in this study; cilengitide (M9173, Abmole, Houston, TX, USA), MG138 (474790, Sigma Aldrich, St. Louis, MO, USA), ferrostatin-1 (SML0583, Sigma Aldrich), necrostatin-1 (ab141053, Abcam, Cambridge, UK), Q-VD-OPH (T0282, TargetMol, Boston, MA, USA), erastin (E7781, Sigma Aldrich), RSL3 (SML2234, Sigma Aldrich), Torin-1 (S2827, Selleck Chemicals, Houston, TX, USA), and cycloheximide (2112S, CST, Danvers, MA, USA).

### 2.2. Cell Lines and Culture Conditions

Human MB cell lines were used in this study. The DAOY cell line (catalog number: HTB-186) was sourced from the American Type Cancer Collection (ATCC, Manassas, VA, USA). The HD-MB03 cell line was acquired from the Deutsche Sammlung von Mikroorganismen und Zellkulturen (DMSZ, Braunschweig, Germany, catalog number: ACC 740). DAOY cells were cultured in Dulbecco's modified eagle medium (DMEM), which was supplemented with 1 mM sodium pyruvate, 2 mM Glutamax, and 7.5% fetal bovine serum (FBS). For HD-MB03 cells, Roswell Park Memorial Institute medium with an additional

7.5% FBS was used. All cell cultures were maintained at 37 °C in a humidified atmosphere with 5% carbon dioxide (CO<sub>2</sub>).

### 2.3. Genetic Disruption of $\beta$ 3-Integrin and Lentiviral Transductions

Generation of  $\beta$ 3-integrin-depleted DAOY and HD-MB03- $\beta$ 3 overexpressing cells were generated in our laboratory as previously described [13].

### 2.4. RT-qPCR

Real-time reverse transcription-quantitative polymerase chain reaction (RT-qPCR) analyses were performed using human MB cell lines. Total mRNAs were isolated using the Nucleospin RNA Kit from Macherey-Nagel (Macherey-Nagel, Düren, Germany). Complementary DNA (cDNA) synthesis was carried out with the Maxima First Strand cDNA Synthesis Kit for RT-qPCR with dsDNase from Thermo Fischer Scientific (Waltham, MA, USA). Quantitative PCR was then performed on an Applied Biosystems StepOnePlus System, using TB Green Premix Ex Ta (Tli RNase H Plus; Takara Bio, San Jose, CA, USA) reagents. Primer sequences included: GPX4\_Forward 5'-GAGGCAAGACCGAAGTAACTAC-3'; GPX4\_Reverse 5'-CCGAAGTGGTTACACGGG-3'. The relative expression levels were calculated by the  $\Delta$ Ct method, with normalization to the reference *36B4* gene.

### 2.5. Immunoblotting

Cells lysis was performed in 1.5× Laemmli buffer, and protein concentrations were quantified with the Pierce BCA Protein Assay from Thermo Fisher Scientific. Protein extracts (15 µg) were subjected to electrophoresis on either 10% or 12% sodium dodecyl-sulfate-polyacrylamide gels and subsequently transferred to polyvinylidene difluoride membranes (Merck Millipore, Burlington, MA, USA). The membranes were blocked with 2% milk in phosphate-buffered saline (PBS) and incubated with the following anti-human antibodies: rabbit anti- $\beta$ 3-integrin (1:1000; 13166, Cell Signaling Technology [CST], Danvers, MA, USA), rabbit anti-xCT (1:1000; 126915, CST), rabbit anti-GPX4 (1:1000; ab125066, Abcam), rabbit anti-p-4EBP1 (1:1000; 1344345, CST), rabbit anti-4EBP1 (1:1000; 9644, CST), rabbit anti-p-70S6K (1:1000; 9202S, CST), rabbit anti-p-RPS6 (1:1000; 2215S, CST), anti-p-paxillin (1:1000; 69363, CST), and rabbit anti-Cyclin D1 (1:1000, ab134175, Abcam). Actin (1:5000; MA5-15739, Thermo Fisher Scientific), Tubulin (1:1000; 2128, CST), and HSP90 (1:1000; MA1-10379, Thermo Scientific) were used as the protein loading control. Immunoreactive bands were detected with horseradish peroxidase-coupled anti-mouse or anti-rabbit antibodies (CST) using the ECL System (Merck Millipore, Burlington, MA, USA).

### 2.6. Irradiation Procedure

Cell irradiation on DAOY-derived and HD-MB03-derived cells was performed using a photon beam of 6 MV delivered by a Varian linear accelerator (Novalis TrueBeam STX (Varian, Palo Alto, CA, USA) using a calibrated irradiation field of 20 × 20 cm<sup>2</sup>. Single doses of 2 to 8 Gy were delivered at 6.5 Gy/min with a 2 cm surface bolus application to ensure dose uniformity at a depth of 100 cm source to tray distance. Non-irradiated cells were given a sham irradiation as controls.

### 2.7. Colony Formation Assay

DAOY-derived and HD-MB03-derived cells were seeded into 60 mm plates after exposure to radiation (0 to 8 Gy) with initial cell numbers of 2000 for DAOY and 4000 cells for HD-MB03-derived cells, respectively. Approximately 10–14 days after seeding, when visible colonies had formed, the cells were washed with phosphate-buffered saline (PBS) and stained with Giemsa solution for 30 min. After staining, the plates were rinsed and air-dried before counting the colonies. Survival fractions were calculated by comparing the colony counts to those of the control cells.

### 2.8. Flow Cytometry

A total of 10,000 events per sample were analyzed using a BD FACSMelody cytometer (Becton Dickinson, Franklin Lakes, NJ, USA), and data was processed using the FlowJo software version vX.0.7 (Ashland, OR, USA). Cells were cultured in 6-well plates at a density of 150,000 cells per well, in triplicate for each condition, and maintained at 37 °C in a 5% CO<sub>2</sub> atmosphere with their respective media. Following this, cells were treated with cilengitide (1 μM) for four hours before exposure to a 2 Gy irradiation, with experiments performed at the indicated time after treatments. Cell death was assessed 48 h following irradiation (2 Gy) using propidium iodide (PI; Invitrogen, Waltham, MA, USA). Both floating and adherent cells were collected, centrifuged, and then resuspended in FACS buffer (PBS, 0.2% BSA, and 2 mM ethylenediaminetetraacetic acid), with 2 μg/mL of PI added just before analysis. Detection of lipid hydroperoxides: MB Cells were seeded in 60 mm diameter dishes and irradiated (2 Gy) 24 h after plating. Another 24 h later, the BODIPY 581/591 C11 dye (Molecular Probes, Eugene, OR, USA) was introduced to the media at a final concentration of 2 μmol/L, and the cells were incubated for 30 min at 37 °C in a 5% CO<sub>2</sub> environment, protected from light. Following incubation, the cells were washed twice with PBS, detached using Accutase (Dutscher, Bernolsheim, France), and resuspended in FACS buffer. The modal scaling option was utilized for data representation, ensuring that each peak is normalized to its mode, corresponding to the percentage of the maximum number of cells within each specific bin.

### 2.9. Statistics

Data are expressed as mean ± standard error of the mean (SEM). Comparisons between groups were conducted using the non-parametric Mann–Whitney test for two groups or two-way analysis of variance (ANOVA) for more than two groups, with multiple comparisons adjusted using Sidak's test. A *p*-value of less than 0.05 was considered statistically significant.

## 3. Results

### 3.1. Integrin- $\alpha$ v $\beta$ 3 Promotes Resistance to IR-Induced Ferroptosis

Two human MB cell lines (DAOY and HD-MB03) were used to investigate the role of integrin- $\alpha$ v $\beta$ 3 in the radiosensitivity of MB. The expression of  $\beta$ 3-integrin was restricted to the DAOY cell line. Genetic depletion or overexpression of  $\beta$ 3-subunit was performed respectively on the DAOY and HD-MB03 cells (Figure 1A,B).

HD-MB03\_LacZ was used as a non-relevant protein expression control for HD-MB03\_ $\beta$ 3+ cells. The generation of these MB-derived cell lines prompted us to analyze the impact of this protein on the radioresistance of MB. Our data clearly showed a decrease in cell survival upon IR in a dose-dependent manner in both DAOY\_WT and KO cells. However, integrin- $\beta$ 3\_KO cells were significantly more sensitive to IR than WT cells at every investigated dose (Figure 1A). Similar results were found in HD-MB03\_LacZ in comparison to HD-MB03\_ $\beta$ 3+ cells, with a significantly higher survival rate for HD-MB03- $\beta$ 3+ at 1 and 2 Gy (Figure 1B).

Next, the type of cell death induced by IR in MB cell lines was investigated using inhibitors of necroptosis, necrostatin-1 (Nec-1); apoptosis, quinolyl-valyl-O-methylaspartyl-[2,6-difluorophenoxy]-methylketone (Q-VD) and ferroptosis, ferrostatin-1 (Fer-1) (Figure 1C,D). As previously observed, a 2 Gy irradiation reduced cell survival to a greater extent in DAOY\_KO cells than in their WT counterparts (81.9% ± 6.9% vs. 28.3% ± 4.6% of cell survival, Figure 1C). Consistently, HD-MB03- $\beta$ 3+ cells displayed a better survival than the control HDMB\_LacZ cells (Figure 1D). Pre-treatment of MB cells with Fer-1 before IR was found to rescue IR-induced cell death in all investigated MB-derived cells (Figure 1C,D). No significant rescue was observed with necroptosis or apoptosis inhibitors, highlighting that cells mainly die of ferroptosis when exposed to IR.

As a major hallmark of ferroptosis, lipid peroxidation was investigated in irradiated MB cell lines. C11-BODIPY staining revealed that 2 Gy IR induced lipid peroxidation exclusively in integrin- $\alpha$ v $\beta$ 3 negative MB cells (Figure 1E,F). Indeed, following irradiation,

lipid hydroperoxides content was four times higher in DAOY\_KO than in DAOY\_WT cells ( $36.3\% \pm 3.4\%$  vs.  $9.8\% \pm 1.8\%$ ) and twice as high in HD-MB03\_LacZ compared to HD-MB03\_β3+ cells ( $20.2\% \pm 1.7\%$  vs.  $9.3\% \pm 1.1\%$ , respectively) (Figure 1E,F). Cell death and lipid peroxide accumulation in DAOY\_KO and HD-MB03\_LacZ 24 h post-irradiation were completely rescued by Fer-1 (Figures 1E,F and S1A,B). Together, our results demonstrated the importance of β3-integrin in responding to IR-induced ferroptosis.

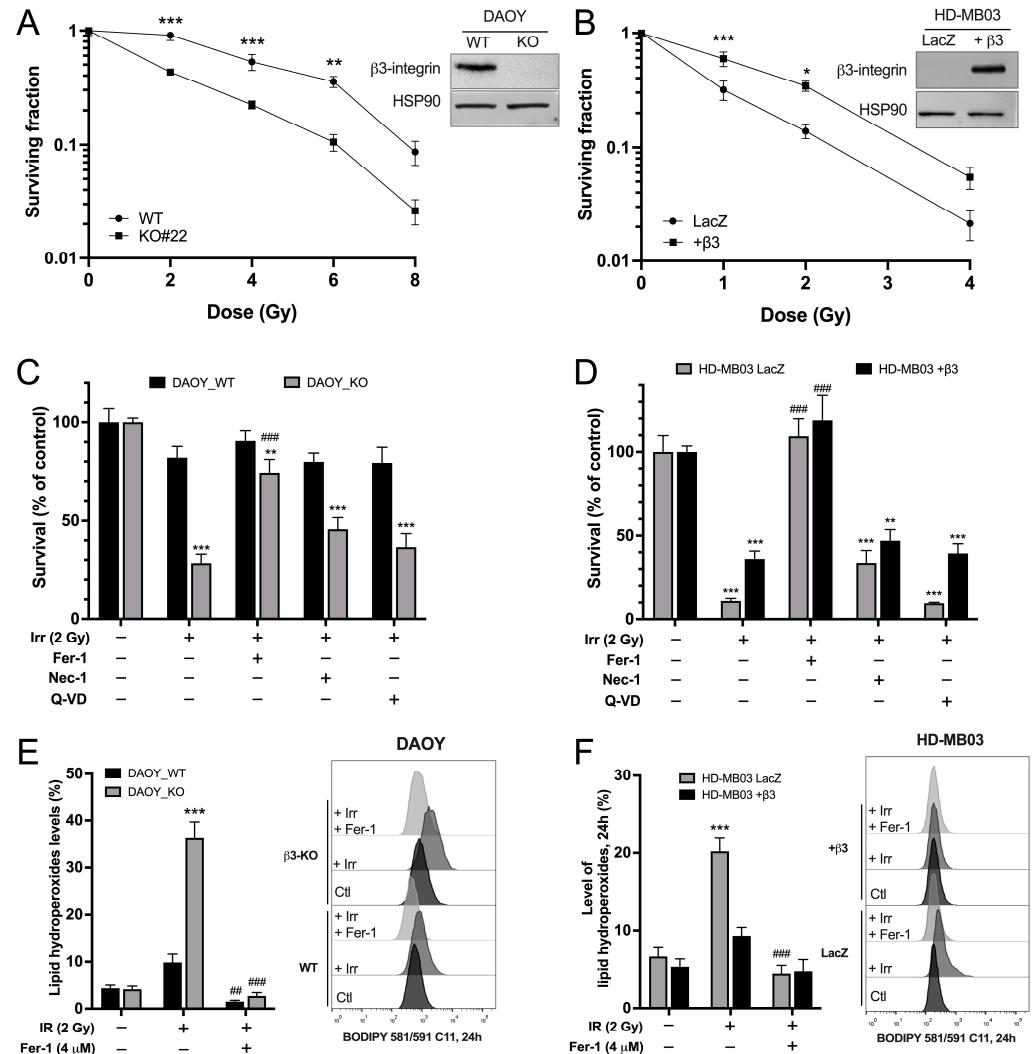


**Figure 1.** β3-depleted MB cells exhibit high sensitivity to IR-induced ferroptosis. (A,B) Representative western blots of β3-integrin expression in DAOY (control vs. β3\_KO) and HD-MB03 (LacZ vs. β3+) cell lines. Survival curves of DAOY\_WT vs. β3\_KO cells (A) and HD-MB03-LacZ vs. HD-MB03-β3+ (B) after a single IR-indicated dose (Gy). Survival was determined by the percentage of unirradiated cells (Log10 scale). \* *p* < 0.05, \*\* *p* < 0.01, \*\*\* *p* < 0.001 vs. corresponding controls. (C,D) Survival fraction of DAOY\_WT and β3\_KO (C) or HD-MB03\_LacZ and +β3 (D) treated with 10 μM necrostatin-1 (Nec-1), 10 μM Q-VD-OPH, or 10 μM ferrostatin-1 (Fer-1) or DMSO (control) and exposed or not to a single dose (2 Gy) of IR. \*\* *p* < 0.01, \*\*\* *p* < 0.001 vs. corresponding control; ### *p* < 0.001 vs. corresponding IR group. (E,F) Lipid hydroperoxide content in DAOY (WT and β3\_KO) and HD-MB03 (LacZ and β3+) cells 24 h after exposure to a 2 Gy IR in the presence or not of Fer-1 (4 μM) measured by C11-BODIPY 581/591 staining. \*\*\* *p* < 0.001 vs. corresponding control; ## *p* < 0.01; ### *p* < 0.001 vs. corresponding IR group. Results are expressed in mean ± SEM. Results are expressed as mean ± SEM. Data points represent three independent biological experiments, with each experiment shown as individual dots. Original uncropped western blot membrane figures can be found in Supplementary File S1.

Given the vulnerability of DAOY\_KO cells to ferroptosis, we hypothesized that targeting GPX4 or xCT could synergize with the depletion of integrin- $\alpha\beta3$ . However, genetic depletion of xCT or GPX4 induces extensive cell death, complicating synergy studies. Pharmacological inhibition allows precise dosing to minimize cell death, enabling the exploration of combinatorial effects with  $\beta3$  inhibition. However, inhibition of GPX4 with RSL3 or xCT with erastin yielded a similar effect on both DAOY\_WT and DAOY\_KO cells (Figure S2A,B). Protein expression analysis in both DAOY-derived cells showed an increased level of xCT upon RSL3 treatment (Figure S2C). Such compensatory mechanisms could account for the lack of cumulative effect of  $\beta3$ -depletion and GPX4 or xCT inhibition on the clonogenic capacities of DAOY cells.

### 3.2. Integrin- $\alpha\beta3$ Regulates Antioxidant Protein Expression

The crucial role of integrin- $\alpha\beta3$  in the resistance of IR-induced ferroptosis prompted us to investigate the underlying molecular mechanisms. The expression of the major components of the antioxidant axis xCT and GPX4 was first assessed in MB-derived cell lines (Figure 2). Levels of both proteins were found to be lower in DAOY\_KO and HD-MB03\_LacZ cells (Figures 2A and S3).

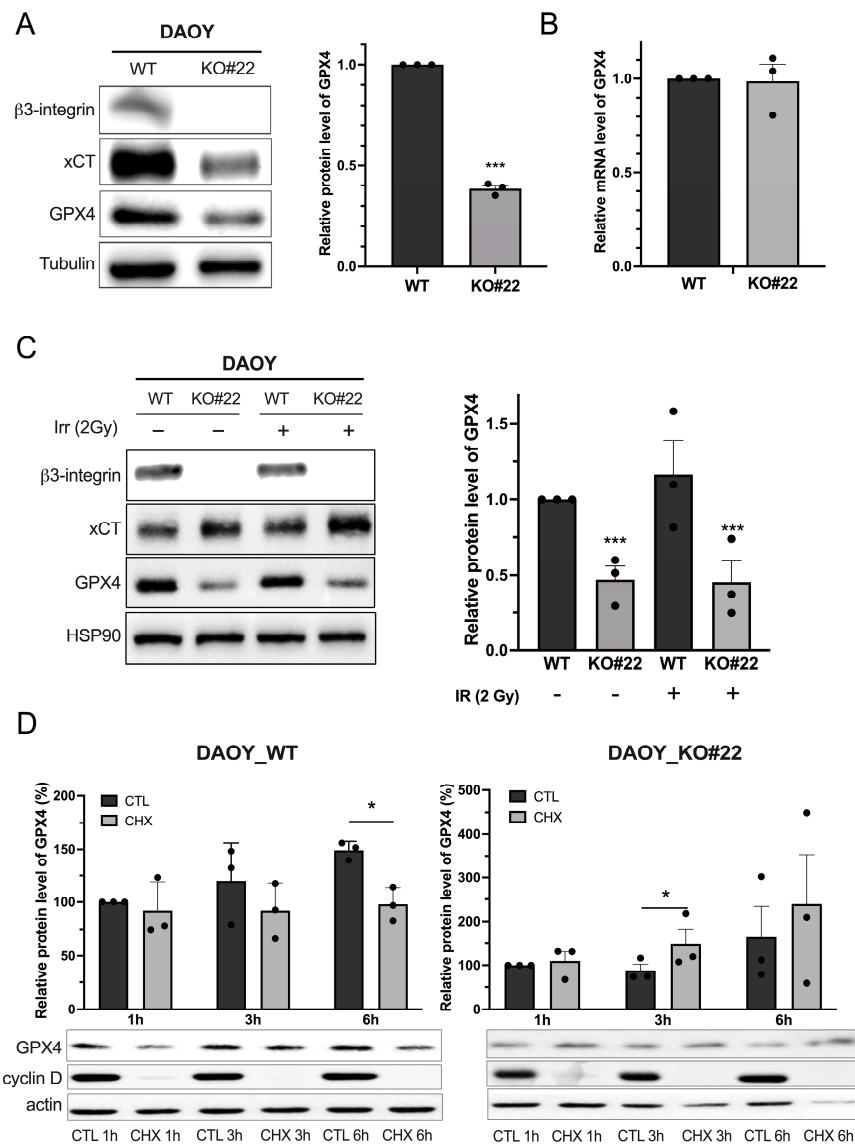


**Figure 2.**  $\beta3$ -depleted MB cells have compromised anti-ferroptotic defense. (A) Protein contents of the major anti-ferroptotic players' xCT and GPX4 were analyzed by Western blot in DAOY (WT and

$\beta 3_{\text{KO}}$ ). Relative GPX4 protein levels are presented as mean  $\pm$  SEM. \*\*\*,  $p < 0.001$  vs. control. (B) Gene expression of GPX4 in DAOY (WT and  $\beta 3_{\text{KO}}$ ) was analyzed by RT-qPCR. Results are expressed in the function of 36B4 gene expression. (C) Protein content of xCT and GPX4 in DAOY (WT and  $\beta 3_{\text{KO}}$ ) was investigated 24 h after a single dose (2 Gy) of IR. Quantification of GPX4 expression is represented on the right panel. \*\*\*,  $p < 0.001$  vs. DAOY\_WT. (D) Cycloheximide (CHX) chase assay for the half-life of GPX4 performed in DAOY\_WT and DAOY  $\beta 3_{\text{KO}}$  cells. Cells were treated with CHX (100  $\mu\text{g}/\text{mL}$ ) for the indicated hours, and Western blotting was performed. The level of remaining GPX4 at different time points was quantified as the percentage of the initial GPX4 level. \*,  $p < 0.05$  vs. corresponding control. Results are expressed in mean  $\pm$  SEM. Results are expressed as mean  $\pm$  SEM. Data points represent three independent biological experiments, with each experiment shown as individual dots. Original uncropped western blot membrane figures can be found in Supplementary File S1.

Specifically, GPX4 protein, a major actor involved in removing lipid hydroperoxides in the plasma membrane, was approximately 70% lower in DAOY\_KO cells in comparison to WT ones (Figure 2A). Similarly, HD-MB03\_  $\beta 3+$  displayed a 50% increase in GPX4 expression compared to HD-MB03\_LacZ (Figure S3). This significant difference persisted post-irradiation, highlighting the strong vulnerability of DAOY\_KO cells to this stress (Figure 2C). On the contrary, xCT expression, a major component of the antioxidative defense, significantly increased following irradiation in DAOY\_WT and DAOY\_KO cells (Figure 2C).

To investigate the influence of integrin- $\alpha\beta 3$  on GPX4 expression, we examined whether this regulation occurs at the transcriptional level. Manipulation of  $\beta 3$  expression levels in both HD-MB03 and DAOY cell lines did not alter GPX4 expression (Figures 2B and S3B). This suggests that  $\beta 3$  integrin is not involved in regulating GPX4 mRNA levels. Additionally, we assessed the effect of integrin- $\alpha\beta 3$  on GPX4 protein stability using a cycloheximide (CHX) chase assay on DAOY-derived cells (Figure 2D). No differences in GPX4 stability were observed under the tested conditions. To further exclude  $\beta 3$  integrin-dependent regulation of GPX4 stability, we investigated proteasome-mediated degradation (Figure S4). Our results indicate that integrin- $\alpha\beta 3$  does not regulate GPX4 protein stability.

### 3.3. Integrin- $\alpha\beta 3$ Regulates GPX4 Expression by Modulating mTORC1 Axis

Given the pivotal role of integrins in cell growth and proliferation and given the fact that GPX4 expression level is not transcriptionally regulated by the integrin- $\alpha\beta 3$  nor through protein stability regulations, we postulated that the signaling from integrin- $\alpha\beta 3$  might globally induce protein translation. mTORC1 is a major cellular hub responsible for protein synthesis. Recent studies in the ferroptosis field have identified mTORC1 as a negative regulator of ferroptosis in cancer cells. Consistent with previous findings, DAOY\_KO cells showed decreased PI3K/Akt and ERK signaling (Figure 3A). Additionally, a significant decrease in mTORC1 downstream phosphorylated targets, such as pS6K, pRPS6, and p4EBP1, was observed in DAOY\_KO cells in comparison to DAOY\_WT cells. Similar results were observed in HD-MB03-derived cells (Figure S5). This decrease was maintained upon irradiation (Figure 3B). To determine if decreased mTORC1 activity affects GPX4 protein levels, the effect of Torin1, a potent and selective ATP-competitive mTOR inhibitor, was evaluated on DAOY cells (Figure 3C). A decrease in phosphorylated-mTORC1 targets was observed at every investigated time point, and GPX4 expression also decreased following a six-hour Torin-1 treatment. Together, our results suggest that mTORC1 pathway activation induces the synthesis of GPX4 (Figure S6).

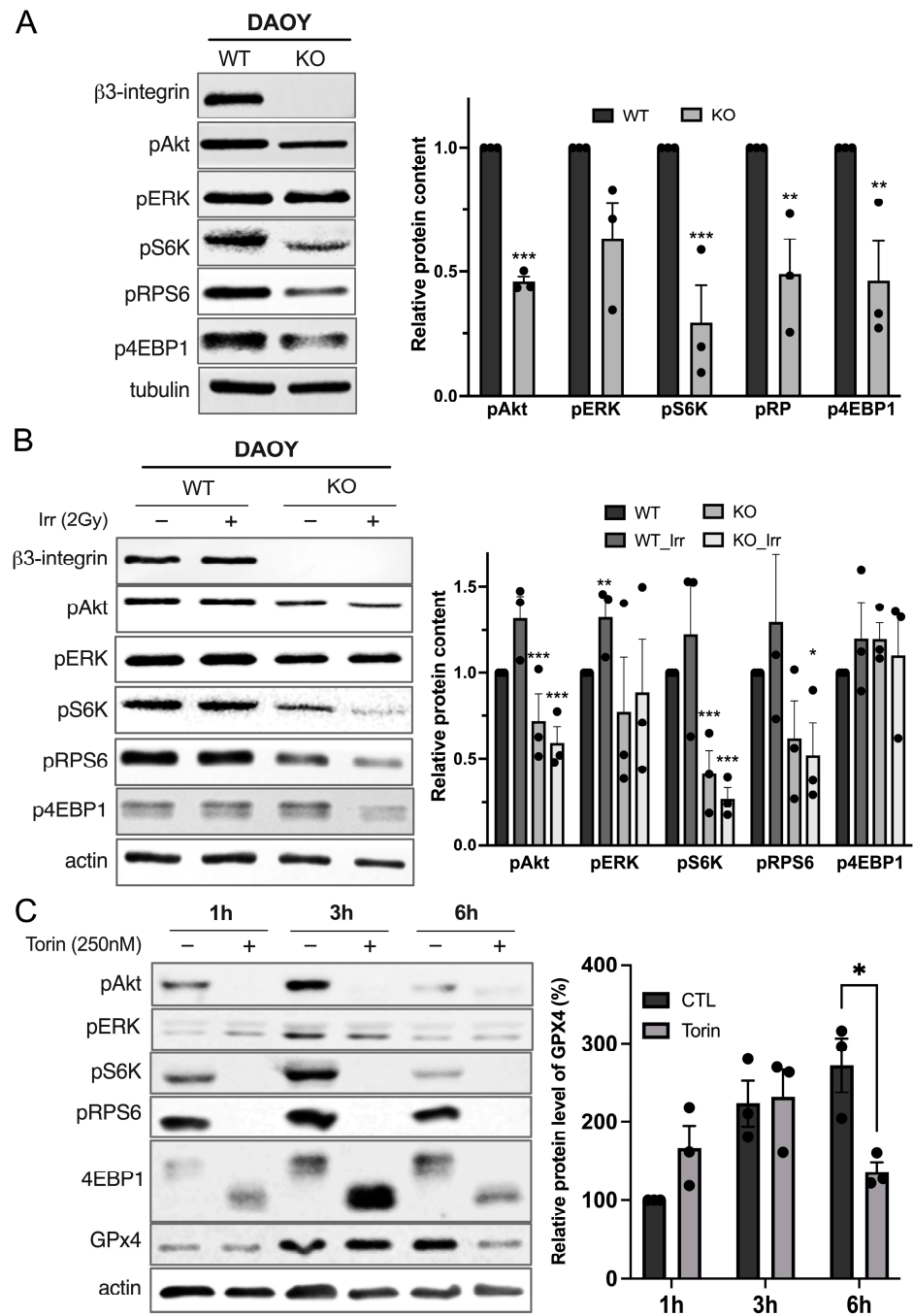


**Figure 3.** Integrin- $\alpha\beta3$  controls GPX4 protein level through its action on mTORC1/4EBP1 axis. (A) Protein levels of  $\alpha\beta3$  signaling, including different cellular targets of mTORC1 complex: 4EBP1, 70S6K, and S6RP, in their phosphorylated form, were measured by Western blot in DAOY. Protein expression in western blots was quantified by densitometry, and the results are expressed in comparison to DAOY\_WT. \*\*,  $p < 0.01$ ; \*\*\*,  $p < 0.001$  vs. DAOY\_WT. (B) Protein levels of  $\alpha\beta3$  signaling were measured by Western blot in DAOY\_WT and DAOY\_β3\_KO 24 h after a 2-Gy IR. Protein expression in western blots was quantified by densitometry, and the results are expressed in comparison to DAOY\_WT. \*,  $p < 0.05$ ; \*\*,  $p < 0.01$ ; \*\*\*,  $p < 0.001$  vs. DAOY\_WT. (C) Protein levels of the indicated protein were measured by Western blot after treatment of DAOY\_WT and DAOY\_β3\_KO after Torin treatment (250 nM, at the indicated time). Protein expression in western blots was quantified by densitometry, and the results are expressed in comparison to control untreated cells. \*,  $p < 0.05$ ; vs. Control. Results are expressed as mean  $\pm$  SEM. Data points represent three independent biological experiments, each shown as individual dots. Original uncropped western blot membrane figures can be found in Supplementary File S1.



### 3.4. Cilengitide Mimics Radiosensitivity Induced by $\beta$ 3-Depletion

To mimic  $\beta$ 3-depletion, we explored the pharmacological impact of cilengitide, an RGD-derived compound, on IR-induced ferroptosis. Pre-treatment of DAOY cells with cilengitide induced a 2-fold increase in cell death after IR compared to the IR-alone group ( $25\% \pm 1.9\%$  vs.  $11.8\% \pm 1.4\%$ ,  $p < 0.001$ ) (Figure S7A). Consistently, an increase of lipid hydroperoxides accumulation was found in cilengitide pre-treated cells after irradiation ( $42.9\% \pm 8.1\%$  vs.  $11.7\% \pm 0.9\%$ ,  $p < 0.01$ , Figure S6B). These effects were totally rescued with the use of Fer-1 (Figure S7A,B). Targeting integrin- $\alpha$  $\beta$ 3, therefore, appears to be an efficient way to increase the sensitivity of MB cells to IR-induced ferroptosis. We next used cilengitide to evaluate the regulation of the mTORC1 axis by integrin- $\alpha$  $\beta$ 3 signaling (Figure S7C). Cilengitide treatment decreased p-paxillin expression, a known downstream target of integrin- $\alpha$  $\beta$ 3, at four hours post-treatment. Disruption of integrin- $\alpha$  $\beta$ 3 signaling led to a significant reduction in p-70S6K, p-RPS6, and p-4EBP1 levels at the same time point. Additionally, a decrease in GPX4 protein content was observed in correlation with these results. Between eight and twenty-four hours of cilengitide treatment, the phosphorylation levels of all investigated proteins and GPX4 protein content were restored (Figure S7C). These results indicate that pharmacological inhibition of integrin- $\alpha$  $\beta$ 3 phenocopies the genetic deletion of its  $\beta$ 3-subunit.

## 4. Discussion

Craniospinal irradiation (CSI) is the cornerstone of MB treatment [5]. Over the past few decades, significant efforts have been made to enhance CSI efficacy, including its combination with chemotherapy. However, relapse and resistance to these therapies underscore the need for new therapeutic strategies. Targeting key pathways of MB resistance, such as those involved in DNA damage response and telomerase activity, represents a promising approach [21–23]. Among alternative targets to overcome tumor radioresistance, integrins have been extensively studied across various cancers and present an attractive option [24]. In line with studies on adult tumors, our previous work demonstrated that integrin- $\alpha$  $\beta$ 3 promotes tumorigenesis and could be a potent therapeutic target for radiosensitization of MB cells [25]. The up-regulation of integrin- $\alpha$  $\beta$ 3 in radioresistant cell lines and their dependency on this complex could open new avenues for this issue.

Healthy and cancerous mammalian tissues are composed of about 70 to 80% water [26]. Therefore, the primary effect of IR imposed on cancerous lesions is water radiolysis, leading to ROS formation and subsequent oxidative damage to nucleic acids, proteins, and membrane lipids [27–29]. Collectively, these effects can induce cell cycle arrest, senescence, and apoptosis [30]. By means of lipid peroxidation measurement and pharmacological rescue, we showed for the first time that radiotherapy primarily induces ferroptosis in  $\beta$ 3-negative MB cells. Since 2012, ferroptosis has been recognized as a novel-ROS-dependent type of cell death, characterized by the accumulation and uncontrolled diffusion of lipid hydroperoxides within the plasma membrane [17]. Despite significant oxidative damage to membrane lipids caused by IR-induced water radiolysis, the role of ferroptosis in radiotherapy was not reported until recently [31]. The first evidence showing the involvement of ferroptosis in response to radiotherapy was recently reported in mouse models of ovarian cancer [32]. Subsequent studies on various tumor types have further confirmed the link between radiotherapy and ferroptosis [33,34]. Consistently, we showed here for the first time that radiotherapy-induced ferroptosis in MB, with integrin- $\alpha$  $\beta$ 3 playing a pivotal role in counterbalancing this process. First, we demonstrated that  $\beta$ 3-depleted cells are more sensitive to radiotherapy compared to  $\beta$ 3-proficient cells. Our data suggest that this increased sensitivity to radiotherapy-induced ferroptosis arises, at least in part, from a compromised anti-ferroptotic antioxidant defense. Our analysis revealed a lower basal level of the canonical players of ferroptosis-preventing pathways, particularly GPX4, in  $\beta$ 3-depleted DAOY and HD-MB03 cells, indicating a compromised internal anti-ferroptotic axis in these cells. Moreover, after radiotherapy,  $\beta$ 3-depleted cells did not show an increase in GPX4 protein levels, in contrast to xCT, which was significantly upregulated

upon radiotherapy in both wild-type and  $\beta 3$ -deficient cells. These results suggest that oxidative stress induced by radiotherapy is sensed by both  $\beta 3$ -proficient and  $\beta 3$ -deficient cell lines, but the latter bears a higher burden of acute oxidative insult, likely due to an insufficient internal antioxidant response. Previous studies on integrin-dependent sensitivity to ferroptosis showed somewhat similar trends. Deletion of integrins such as  $\alpha v\beta 3$  or  $\alpha 6\beta 4$  increases cell sensitivity to ferroptosis, partly due to loss of xCT stability or increased synthesis of polyunsaturated fatty acids by the enzyme Acyl-CoA Synthetase Long-Chain Family Member 4 (ACSL4) [35,36]. Interestingly, in both studies, the deletion of integrins also led to a reduction in GPX4 protein levels, a point that was not addressed by the authors. Considering the absence of influence of  $\beta 3$ -integrin on GPX4 mRNA levels and GPX4 protein stability (as seen in CHX chase experiments), we hypothesized that integrin- $\alpha v\beta 3$  regulates its expression by influencing protein synthesis. We previously demonstrated that integrin- $\alpha v\beta 3$  induces activation of Akt, a positive regulator of the major protein synthesis regulator, mTORC1. Consistent with these results, we showed that disruption of integrin- $\alpha v\beta 3$  signaling decreased mTORC1 activity, as reflected by the reduced phosphorylation of S6K and 4EBP1. These findings align with data showing the impact of other integrins on mTORC1 activity [37,38]. To our knowledge, this is the first time that the AKT/mTORC1/4EBP1/GPX4 axis has been investigated downstream of the integrin- $\alpha v\beta 3$  signaling.

The data presented here also address an important and still controversial question: the regulation of GPX4 expression. One frequently mentioned regulator of GPX4 is nuclear factor erythroid 2-related factor 2 (NRF2), a well-known sensor of the cellular redox state [39–41]. However, our previous studies suggest that this might not be the case. In xCT-depleted cells experiencing high oxidative stress and increased NRF2 signaling, the content of GPX4 remained markedly lower compared to their WT counterparts [42]. According to two recent studies on GPX4 regulation, a potential reason for this might be the suppressed activity of mTORC1 observed in cells upon cysteine starvation [43,44]. To investigate this issue, we treated the cells with Torin-1, a selective ATP-competitive mTORC1 inhibitor. Here, mTORC1 inhibition correlates with decreased GPX4 protein levels four hours after treatment. Torin-1 induced incomplete dephosphorylation of 70S6K and RPS6. However, a complete decrease of 4EBP1 phosphorylation, a “good quality” substrate of mTORC1, was found upon Torin-1 treatment. This result suggests that this branch of mTORC1 might be responsible for the protein synthesis of GPX4. 4EBP1 acts as a scavenger of eIF4E. When 4EBP1 is phosphorylated by mTORC1, eIF4E participates in recognizing the stabilizer CAP (m7GpppNm) present at the 5' end of the mRNA, allowing the translation initiation of proteins such as GPX4. This aligns with Zhang et al.'s study, which showed that GPX4 is regulated by a Rag-mTORC1-4EBP1 axis. Interestingly, despite the proven efficacy of these inhibitors, GPX4 protein levels began to increase post-treatment of eight hours and were fully restored by 24 h, likely due to cellular adaptation to pharmacological mTORC1 inhibition (Figure S5).

We used cilengitide, an RGD-derived compound, to validate through a pharmacological approach the data generated by the genetic depletion of  $\beta 3$ -integrin. Cilengitide has shown promise as a therapeutic compound due to its anti-tumor effects and ability to pass the blood-brain barrier [45–47]. We observed a decrease in GPX4 expression and mTORC1 activity starting four hours after cilengitide treatment. This finding aligns with the radiosensitizing effect of cilengitide. Moreover, our data underscore the necessity of precise timing for drug administration, considering that GPX4 levels and mTORC1 activity were restored from eight hours and further increased after 24 h, suggesting a compensatory mechanism like the one observed with torin-1. The transient nature of cilengitide's effects on GPX4 and mTORC1 activities suggests that its therapeutic window is narrow, necessitating careful consideration of dosing schedules to sustain its anti-tumor effects. While the in vitro half-life of cilengitide is unknown, clinical studies report a plasma half-life of 3–5 h post-intravenous infusion [48]. In an orthotopic model of glioma, administering cilengitide shortly before radiotherapy was found to enhance tumor response, demonstrating

the importance of treatment scheduling [48]. Additionally, further investigation into the compensatory mechanisms that restore GPX4 and mTORC1 activities post-treatment could reveal new targets for enhancing the efficacy of cilengitide in clinical settings.

In conclusion, our findings underscore the therapeutic potential of targeting integrin- $\alpha\text{v}\beta\text{3}$  and the mTORC1/GPX4 pathway to induce ferroptosis and overcome radioresistance in MB. To the best of our knowledge, this is the first study that demonstrated the impact of integrin- $\alpha\text{v}\beta\text{3}$  in radiotherapy-induced ferroptosis.

**Supplementary Materials:** The following supporting information can be downloaded at: <https://www.mdpi.com/article/10.3390/curroncol31110545/s1>, Figure S1:  $\beta\text{3}$ -depleted MB cells are sensitive to IR-induced ferroptosis; Figure S2:  $\beta\text{3}$ -proficient and deficient DAOY cells show the same sensitivity to ferroptosis inducers; Figure S3: Overexpression of  $\beta\text{3}$  in HD-MB03 increases GPX4 protein expression; Figure S4: Proteasome inhibition assay in DAOY-derived cells; Figure S5: Integrin- $\alpha\text{v}\beta\text{3}$  controls GPX4 protein level through its action on mTORC1/4EBP1 axis; Figure S6: Schematic representation of the hypothetical regulation of GPX4 protein synthesis by integrin- $\alpha\text{v}\beta\text{3}$  signalization; Figure S7: Pharmacological inhibition of integrin- $\alpha\text{v}\beta\text{3}$  by cilengitide phenocopies radiosensitivity of the genetic  $\beta\text{3}$ -deletion; File S1: Original uncropped western blot membrane figures.

**Author Contributions:** Conceptualization, M.V. and C.M.; methodology, B.S., V.P., M.V. and C.M.; software, C.G., M.V. and C.M.; validation, V.P., M.V. and C.M.; formal analysis, C.G., F.S., W.E., J.D., T.B., C.O., B.S., V.P., M.V. and C.M.; investigation, C.G., F.S., W.E., J.D., T.B., V.V., M.P.-B., R.V., R.A., N.G., C.O., B.S., V.P., M.V. and C.M.; resources, J.P., V.P., M.V. and C.M.; data curation, C.G., F.S., W.E., J.D., T.B., V.V., M.P.-B., R.V., R.A., N.G., C.O. and B.S.; writing—original draft preparation, C.G.; writing—review and editing, C.G., V.P., M.V. and C.M.; visualization, C.G., F.S., W.E., M.V. and C.M.; supervision, V.P., M.V. and C.M.; funding acquisition, J.P., V.P., M.V. and C.M. All authors have read and agreed to the published version of the manuscript.

**Funding:** This research was funded by the Government of the Principality of Monaco, Fondation Flavien, AS Monaco FC, and Groupement des Entreprises Monégasques dans la Lutte contre le Cancer (GEMLUC).

**Institutional Review Board Statement:** Not applicable.

**Informed Consent Statement:** Not applicable.

**Data Availability Statement:** All the datasets shown in the figures are available from the corresponding author upon reasonable request.

**Acknowledgments:** The authors are extremely grateful to all the staff members of Fondation Flavien and GEMLUC for their constant efforts and strong support.

**Conflicts of Interest:** The authors declare no conflicts of interest.

## References

1. Johnson, K.J.; Cullen, J.; Barnholtz-Sloan, J.S.; Ostrom, Q.T.; Langer, C.E.; Turner, M.C.; McKean-Cowdin, R.; Fisher, J.L.; Lupo, P.J.; Partap, S.; et al. Childhood Brain Tumor Epidemiology: A Brain Tumor Epidemiology Consortium Review. *Cancer Epidemiol. Biomark. Prev.* **2014**, *23*, 2716–2736. [[CrossRef](#)] [[PubMed](#)]
2. Louis, D.N.; Perry, A.; Reifenberger, G.; von Deimling, A.; Figarella-Branger, D.; Cavenee, W.K.; Ohgaki, H.; Wiestler, O.D.; Kleihues, P.; Ellison, D.W. The 2016 World Health Organization Classification of Tumors of the Central Nervous System: A Summary. *Acta Neuropathol.* **2016**, *131*, 803–820. [[CrossRef](#)] [[PubMed](#)]
3. Louis, D.N.; Perry, A.; Wesseling, P.; Brat, D.J.; Cree, I.A.; Figarella-Branger, D.; Hawkins, C.; Ng, H.K.; Pfister, S.M.; Reifenberger, G.; et al. The 2021 WHO Classification of Tumors of the Central Nervous System: A Summary. *Neuro. Oncol.* **2021**, *23*, 1231–1251. [[CrossRef](#)]
4. Padovani, L.; Horan, G.; Ajithkumar, T. Radiotherapy Advances in Paediatric Medulloblastoma Treatment. *Clin. Oncol. (R. Coll. Radiol.)* **2019**, *31*, 171–181. [[CrossRef](#)]
5. Seidel, C.; Heider, S.; Hau, P.; Glasow, A.; Dietzsch, S.; Kortmann, R.-D. Radiotherapy in Medulloblastoma-Evolution of Treatment, Current Concepts and Future Perspectives. *Cancers* **2021**, *13*, 5945. [[CrossRef](#)]
6. Chevignard, M.; Câmara-Costa, H.; Doz, F.; Dellatolas, G. Core Deficits and Quality of Survival after Childhood Medulloblastoma: A Review. *Neurooncol. Pract.* **2017**, *4*, 82–97. [[CrossRef](#)]
7. Pizer, B.L.; Clifford, S.C. The Potential Impact of Tumour Biology on Improved Clinical Practice for Medulloblastoma: Progress towards Biologically Driven Clinical Trials. *Br. J. Neurosurg.* **2009**, *23*, 364–375. [[CrossRef](#)]

8. Jakacki, R.I.; Burger, P.C.; Zhou, T.; Holmes, E.J.; Kocak, M.; Onar, A.; Goldwein, J.; Mehta, M.; Packer, R.J.; Tarbell, N.; et al. Outcome of Children With Metastatic Medulloblastoma Treated With Carboplatin During Craniospinal Radiotherapy: A Children’s Oncology Group Phase I/II Study. *J. Clin. Oncol.* **2012**, *30*, 2648–2653. [[CrossRef](#)] [[PubMed](#)]
9. Hill, R.M.; Richardson, S.; Schwalbe, E.C.; Hicks, D.; Lindsey, J.C.; Crosier, S.; Rafiee, G.; Grabovska, Y.; Wharton, S.B.; Jacques, T.S.; et al. Time, Pattern, and Outcome of Medulloblastoma Relapse and Their Association with Tumour Biology at Diagnosis and Therapy: A Multicentre Cohort Study. *Lancet Child Adolesc. Health* **2020**, *4*, 865–874. [[CrossRef](#)]
10. Ferreira, S.; Foray, C.; Gatto, A.; Larcher, M.; Heinrich, S.; Lupu, M.; Mispelter, J.; Boussin, F.D.; Pouponnot, C.; Dutreix, M. AsiDNA Is a Radiosensitizer with No Added Toxicity in Medulloblastoma Pediatric Models. *Clin. Cancer Res.* **2020**, *26*, 5735–5746. [[CrossRef](#)]
11. Douyère, M.; Gong, C.; Richard, M.; Pellegrini-Moïse, N.; Daouk, J.; Pierson, J.; Chastagner, P.; Boura, C. NRP1 Inhibition Modulates Radiosensitivity of Medulloblastoma by Targeting Cancer Stem Cells. *Cancer Cell Int.* **2022**, *22*, 377. [[CrossRef](#)] [[PubMed](#)]
12. Buck, J.; Dyer, P.J.C.; Hii, H.; Carline, B.; Kuchibhotla, M.; Byrne, J.; Howlett, M.; Whitehouse, J.; Ebert, M.A.; McDonald, K.L.; et al. Veliparib Is an Effective Radiosensitizing Agent in a Preclinical Model of Medulloblastoma. *Front. Mol. Biosci.* **2021**, *8*, 633344. [[CrossRef](#)] [[PubMed](#)]
13. Echavidre, W.; Durivault, J.; Gotorbe, C.; Blanchard, T.; Pagnuzzi, M.; Vial, V.; Raes, F.; Broisat, A.; Villeneuve, R.; Amblard, R.; et al. Integrin-Av $\beta$ 3 Is a Therapeutically Targetable Fundamental Factor in Medulloblastoma Tumorigenicity and Radioresistance. *Cancer Res. Commun.* **2023**, *3*, 2483–2496. [[CrossRef](#)]
14. Takada, Y.; Ye, X.; Simon, S. The Integrins. *Genome Biol.* **2007**, *8*, 215. [[CrossRef](#)] [[PubMed](#)]
15. Ellert-Miklaszewska, A.; Poleszak, K.; Pasierbinska, M.; Kaminska, B. Integrin Signaling in Glioma Pathogenesis: From Biology to Therapy. *Int. J. Mol. Sci.* **2020**, *21*, 888. [[CrossRef](#)]
16. Echavidre, W.; Picco, V.; Faraggi, M.; Montemagno, C. Integrin-Av $\beta$ 3 as a Therapeutic Target in Glioblastoma: Back to the Future? *Pharmaceutics* **2022**, *14*, 1053. [[CrossRef](#)]
17. Dixon, S.J.; Lemberg, K.M.; Lamprecht, M.R.; Skouta, R.; Zaitsev, E.M.; Gleason, C.E.; Patel, D.N.; Bauer, A.J.; Cantley, A.M.; Yang, W.S.; et al. Ferroptosis: An Iron-Dependent Form of Nonapoptotic Cell Death. *Cell* **2012**, *149*, 1060–1072. [[CrossRef](#)]
18. Ursini, F.; Maiorino, M.; Gregolin, C. The Selenoenzyme Phospholipid Hydroperoxide Glutathione Peroxidase. *Biochim. Et Biophys. Acta (BBA) Gen. Subj.* **1985**, *839*, 62–70. [[CrossRef](#)]
19. Yang, W.S.; SriRamaratnam, R.; Welsch, M.E.; Shimada, K.; Skouta, R.; Viswanathan, V.S.; Cheah, J.H.; Clemons, P.A.; Shamji, A.F.; Clish, C.B.; et al. Regulation of Ferroptotic Cancer Cell Death by GPX4. *Cell* **2014**, *156*, 317–331. [[CrossRef](#)]
20. Daher, B.; Vučetić, M.; Pouysségur, J. Cysteine Depletion, a Key Action to Challenge Cancer Cells to Ferroptotic Cell Death. *Front. Oncol.* **2020**, *10*, 723. [[CrossRef](#)]
21. Endersby, R.; Whitehouse, J.; Pribnow, A.; Kuchibhotla, M.; Hii, H.; Carline, B.; Gande, S.; Stripay, J.; Ancliffe, M.; Howlett, M.; et al. Small-Molecule Screen Reveals Synergy of Cell Cycle Checkpoint Kinase Inhibitors with DNA-Damaging Chemotherapies in Medulloblastoma. *Sci. Transl. Med.* **2021**, *13*, eaba7401. [[CrossRef](#)] [[PubMed](#)]
22. Nakamura, M.; Masutomi, K.; Kyo, S.; Hashimoto, M.; Maida, Y.; Kanaya, T.; Tanaka, M.; Hahn, W.C.; Inoue, M. Efficient Inhibition of Human Telomerase Reverse Transcriptase Expression by RNA Interference Sensitizes Cancer Cells to Ionizing Radiation and Chemotherapy. *Hum. Gene Ther.* **2005**, *16*, 859–868. [[CrossRef](#)]
23. Patties, I.; Kortmann, R.-D.; Menzel, F.; Glasow, A. Enhanced Inhibition of Clonogenic Survival of Human Medulloblastoma Cells by Multimodal Treatment with Ionizing Irradiation, Epigenetic Modifiers, and Differentiation-Inducing Drugs. *J. Exp. Clin. Cancer Res.* **2016**, *35*, 94. [[CrossRef](#)]
24. Bergonzini, C.; Kroese, K.; Zweemer, A.J.M.; Danen, E.H.J. Targeting Integrins for Cancer Therapy—Disappointments and Opportunities. *Front. Cell Dev. Biol.* **2022**, *10*, 863850. [[CrossRef](#)]
25. Pachane, B.C.; Selistre-de-Araujo, H.S. The Role of Av $\beta$ 3 Integrin in Cancer Therapy Resistance. *Biomedicines* **2024**, *12*, 1163. [[CrossRef](#)] [[PubMed](#)]
26. Penet, M.-F.; Kakkad, S.; Wildes, F.; Bhujwalla, Z.M. Water and Collagen Content Are High in Pancreatic Cancer: Implications for Quantitative Metabolic Imaging. *Front. Oncol.* **2020**, *10*, 599204. [[CrossRef](#)]
27. Lu, Z.; Zheng, X.; Ding, C.; Zou, Z.; Liang, Y.; Zhou, Y.; Li, X. Deciphering the Biological Effects of Radiotherapy in Cancer Cells. *Biomolecules* **2022**, *12*, 1167. [[CrossRef](#)] [[PubMed](#)]
28. Liu, R.; Bian, Y.; Liu, L.; Liu, L.; Liu, X.; Ma, S. Molecular Pathways Associated with Oxidative Stress and Their Potential Applications in Radiotherapy (Review). *Int. J. Mol. Med.* **2022**, *49*, 65. [[CrossRef](#)]
29. Azzam, E.I.; Jay-Gerin, J.-P.; Pain, D. Ionizing Radiation-Induced Metabolic Oxidative Stress and Prolonged Cell Injury. *Cancer Lett.* **2012**, *327*, 48–60. [[CrossRef](#)]
30. Adjemian, S.; Oltean, T.; Martens, S.; Wiernicki, B.; Goossens, V.; Vanden Berghe, T.; Cappe, B.; Ladik, M.; Riquet, F.B.; Heyndrickx, L.; et al. Ionizing Radiation Results in a Mixture of Cellular Outcomes Including Mitotic Catastrophe, Senescence, Methuosis, and Iron-Dependent Cell Death. *Cell Death Dis.* **2020**, *11*, 1003. [[CrossRef](#)]
31. Haimovitz-Friedman, A.; Kan, C.C.; Ehleiter, D.; Persaud, R.S.; McLoughlin, M.; Fuks, Z.; Kolesnick, R.N. Ionizing Radiation Acts on Cellular Membranes to Generate Ceramide and Initiate Apoptosis. *J. Exp. Med.* **1994**, *180*, 525–535. [[CrossRef](#)] [[PubMed](#)]

32. Lang, X.; Green, M.D.; Wang, W.; Yu, J.; Choi, J.E.; Jiang, L.; Liao, P.; Zhou, J.; Zhang, Q.; Dow, A.; et al. Radiotherapy and Immunotherapy Promote Tumoral Lipid Oxidation and Ferroptosis via Synergistic Repression of SLC7A11. *Cancer Discov.* **2019**, *9*, 1673–1685. [[CrossRef](#)] [[PubMed](#)]
33. Ye, L.F.; Chaudhary, K.R.; Zandkarimi, F.; Harken, A.D.; Kinslow, C.J.; Upadhyayula, P.S.; Dovas, A.; Higgins, D.M.; Tan, H.; Zhang, Y.; et al. Radiation-Induced Lipid Peroxidation Triggers Ferroptosis and Synergizes with Ferroptosis Inducers. *ACS Chem. Biol.* **2020**, *15*, 469–484. [[CrossRef](#)]
34. Zhang, Z.; Lu, M.; Chen, C.; Tong, X.; Li, Y.; Yang, K.; Lv, H.; Xu, J.; Qin, L. Holo-Lactoferrin: The Link between Ferroptosis and Radiotherapy in Triple-Negative Breast Cancer. *Theranostics* **2021**, *11*, 3167–3182. [[CrossRef](#)] [[PubMed](#)]
35. Li, F.; Xu, T.; Chen, P.; Sun, R.; Li, C.; Zhao, X.; Ou, J.; Li, J.; Liu, T.; Zeng, M.; et al. Platelet-Derived Extracellular Vesicles Inhibit Ferroptosis and Promote Distant Metastasis of Nasopharyngeal Carcinoma by Upregulating ITGB3. *Int. J. Biol. Sci.* **2022**, *18*, 5858–5872. [[CrossRef](#)]
36. Brown, C.W.; Amante, J.J.; Goel, H.L.; Mercurio, A.M. The A $\beta$ 4 Integrin Promotes Resistance to Ferroptosis. *J. Cell Biol.* **2017**, *216*, 4287–4297. [[CrossRef](#)]
37. Soung, Y.H.; Korneeva, N.; Kim, T.H.; Chung, J. The Role of C-Src in Integrin (A $\beta$ 4) Dependent Translational Control. *BMC Cell Biol.* **2013**, *14*, 49. [[CrossRef](#)]
38. Mousavizadeh, R.; Hojabrpour, P.; Eltit, F.; McDonald, P.C.; Dedhar, S.; McCormack, R.G.; Duronio, V.; Jafarnejad, S.M.; Scott, A. B1 Integrin, ILK and mTOR Regulate Collagen Synthesis in Mechanically Loaded Tendon Cells. *Sci. Rep.* **2020**, *10*, 12644. [[CrossRef](#)]
39. Osburn, W.O.; Wakabayashi, N.; Misra, V.; Nilles, T.; Biswal, S.; Trush, M.A.; Kensler, T.W. Nrf2 Regulates an Adaptive Response Protecting against Oxidative Damage Following Diquat-Mediated Formation of Superoxide Anion. *Arch. Biochem. Biophys.* **2006**, *454*, 7–15. [[CrossRef](#)]
40. Zhao, J.; Tang, P.; Zhou, Z.; Xu, G.; Li, Q.; Li, K.; Zheng, Y. Nrf2 Signaling Activation by a Small Molecule Activator Compound 16 Inhibits Hydrogen Peroxide-Induced Oxidative Injury and Death in Osteoblasts. *Cell Death Discov.* **2022**, *8*, 353. [[CrossRef](#)]
41. Dodson, M.; Castro-Portuguez, R.; Zhang, D.D. NRF2 Plays a Critical Role in Mitigating Lipid Peroxidation and Ferroptosis. *Redox Biol.* **2019**, *23*, 101107. [[CrossRef](#)] [[PubMed](#)]
42. Daher, B.; Parks, S.K.; Durivault, J.; Cormerais, Y.; Baidarjad, H.; Tambutte, E.; Pouysségur, J.; Vučetić, M. Genetic Ablation of the Cystine Transporter xCT in PDAC Cells Inhibits mTORC1, Growth, Survival, and Tumor Formation via Nutrient and Oxidative Stresses. *Cancer Res.* **2019**, *79*, 3877–3890. [[CrossRef](#)] [[PubMed](#)]
43. Zhang, Y.; Swanda, R.V.; Nie, L.; Liu, X.; Wang, C.; Lee, H.; Lei, G.; Mao, C.; Koppula, P.; Cheng, W.; et al. mTORC1 Couples Cyst(e)ine Availability with GPX4 Protein Synthesis and Ferroptosis Regulation. *Nat. Commun.* **2021**, *12*, 1589. [[CrossRef](#)]
44. Cai, J.; Ye, Z.; Hu, Y.; Ye, L.; Gao, L.; Wang, Y.; Sun, Q.; Tong, S.; Zhang, S.; Wu, L.; et al. Fatostatin Induces Ferroptosis through Inhibition of the AKT/mTORC1/GPX4 Signaling Pathway in Glioblastoma. *Cell Death Dis.* **2023**, *14*, 211. [[CrossRef](#)] [[PubMed](#)]
45. Stupp, R.; Hegi, M.E.; Neyns, B.; Goldbrunner, R.; Schlegel, U.; Clement, P.M.J.; Grabenbauer, G.G.; Ochsenein, A.F.; Simon, M.; Dietrich, P.-Y. Phase I/IIa Study of Cilengitide and Temozolomide with Concomitant Radiotherapy Followed by Cilengitide and Temozolomide Maintenance Therapy in Patients with Newly Diagnosed Glioblastoma. *J. Clin. Oncol. Off. J. Am. Soc. Clin. Oncol.* **2010**, *28*, 2712–2718. [[CrossRef](#)]
46. Weller, M.; Nabors, L.B.; Gorlia, T.; Leske, H.; Rushing, E.; Bady, P.; Hicking, C.; Perry, J.; Hong, Y.-K.; Roth, P. Cilengitide in Newly Diagnosed Glioblastoma: Biomarker Expression and Outcome. *Oncotarget* **2016**, *7*, 15018–15032. [[CrossRef](#)]
47. Kim, Y.-H.; Lee, J.K.; Kim, B.; DeWitt, J.P.; Lee, J.E.; Han, J.H.; Kim, S.-K.; Oh, C.W.; Kim, C.-Y. Combination Therapy of Cilengitide with Belotecan against Experimental Glioblastoma. *Int. J. Cancer* **2013**, *133*, 749–756. [[CrossRef](#)]
48. Mikkelsen, T.; Brodie, C.; Finniss, S.; Berens, M.E.; Rennert, J.L.; Nelson, K.; Lemke, N.; Brown, S.L.; Hahn, D.; Neuteboom, B.; et al. Radiation Sensitization of Glioblastoma by Cilengitide Has Unanticipated Schedule-Dependency. *Int. J. Cancer* **2009**, *124*, 2719–2727. [[CrossRef](#)]

**Disclaimer/Publisher’s Note:** The statements, opinions and data contained in all publications are solely those of the individual author(s) and contributor(s) and not of MDPI and/or the editor(s). MDPI and/or the editor(s) disclaim responsibility for any injury to people or property resulting from any ideas, methods, instructions or products referred to in the content.